

## International Journal of Engineering Research and Development

DOI: 10.29137/ijerad.1674277



Volume:17 Issue:03 Pages:590-603 November/2025

Research Article

# In vitro evaluation of the antineoplastic activity of silver nanoparticles functionalized with bioactive molecules against SK-MEL-30, MCF-7, and H1299 cancer cells

Esra Bozkava 1,2

<sup>1</sup>Scientific and Technological Researches Application and Research Center, Kırıkkale University, 71450 Kırıkkale, TURKEY <sup>2</sup>Property Protection and Security Department, Hüseyin Aytemiz Vocational High School, Kırıkkale University, 71450 Kırıkkale, TURKEY

**Final Version**: 30/11/2025

#### Abstract

The present study aimed to evaluate the in vitro antineoplastic activity of silver nanoparticles (AgNPs) biosynthesized using *Centella asiatica* (CA) leaf extract against human SK-MEL-30 skin cancer, MCF-7 breast cancer, and H1299 lung cancer cell lines. CA/AgNPs were synthesized via a green chemistry approach and characterized by standard physicochemical techniques. The anticancer potential of the synthesized nanoparticles was assessed using MTT assays, along with apoptotic and necrotic index evaluations. Results indicated a dose-dependent reduction in cell viability in all cancer cell lines, while minimal cytotoxicity was observed in normal L929 fibroblast cells. Notably, CA and CA/AgNPs induced apoptosis and necrosis selectively in cancer cells, suggesting that both formulations possess strong antitumoral effects. The apoptotic indices were especially high in H1299 lung cancer cells treated with CA extract, whereas necrosis was most pronounced in SK-MEL-30 cells at higher concentrations. Taken together, these findings support the antineoplastic, anticancer, and cytotoxic potential of CA/AgNPs, highlighting their promise as biocompatible agents for targeted cancer therapies. Further in vivo studies are recommended to validate these effects.

## Keywords

Antineoplastic activity, silver nanoparticle, Centella asiatica, anticancer activity, apoptosis induction, green synthesis

<sup>\*</sup> Corresponding Author: esraarat@kku.edu.tr

## 1. Introduction

In recent years, the rapid increase in cancer incidence worldwide has made the development of new therapeutic approaches an urgent necessity. This growing prevalence has driven scientists to improve existing treatment strategies and to explore alternative approaches that are more effective and less toxic. Cancer is treated using various methods, including chemotherapy, hormone therapy, radiotherapy, immunotherapy, photodynamic therapy, stem cell transplantation, targeted therapy, and surgery (NCI) (Şahin et al., 2023). Among these treatment modalities, chemotherapy remains one of the most widely used approaches. Accordingly, research efforts have intensified to enhance the efficacy of existing drugs and to identify novel compounds with anticancer potential. Scientists continue to investigate the potential effects of known compounds on complex diseases such as cancer, with particular attention given to naturally derived substances. In recent years, there has been a marked increase in studies highlighting the role of natural compounds in cancer therapy, as these substances are regarded as promising therapeutic agents (Wiciński et al., 2024). Approximately half a century of systemic drug discovery and development has led to the creation of numerous effective chemotherapeutic agents. However, chemotherapeutic treatments are associated with significant drawbacks. The administration of these therapies can result in various toxicities and adverse effects. According to the literature, several commonly used chemotherapeutic agents have been reported to be associated with myelotoxicity, cardiotoxicity, nephrotoxicity, pulmonary toxicity, hemorrhagic cystitis, immunosuppression, alopecia, and bladder toxicity (Cohen et al., 1973; Gibaud et al., 1994; Macdonald, 1999; Manil et al., 1995; Rexroth & Scotland, 1994). These adverse effects have driven research towards alternative and supportive treatment approaches. In recent years, there has been a growing interest in the use of plant-derived compounds in cancer therapy. Bioactive molecules extracted from plants have demonstrated significant anticancer properties and have served as the foundation for the development of chemotherapeutic agents. Notably, plantderived chemotherapeutic drugs such as paclitaxel (Taxol), vinblastine, vincristine, camptothecin, and etoposide have been successfully introduced into clinical use, achieving substantial efficacy in cancer treatment (Desai et al., 2008). Additionally, phytochemicals such as polyphenols, flavonoids, alkaloids, and terpenoids have been recognized for their immunomodulatory and antioxidant properties, making them valuable candidates as adjunctive agents in cancer therapy. Current research explores the efficacy and toxicity profiles of plant-based molecules in targeted cancer therapies, as well as their potential for integration with chemotherapy and immunotherapy (Yırtıcı et al., 2024). In this context, the discovery of plant-derived anticancer agents represents a crucial area of investigation in pharmaceutical and oncological sciences. Currently, more than 60% of anticancer agents used in cancer treatment are derived from natural sources, such as plants. According to Hartwell's studies, over 3,000 plant species have been reported to exhibit anticancer properties (Graham et al., 2000).

Centella asiatica (CA) is a plant that has been used for centuries in Asian countries, primarily for the treatment of wounds, burns, and skin diseases (O. Bozkaya et al., 2023). Today, its reputation has spread to many countries around the world. This ancient plant, which can be found in the sources of various ancient civilizations (Gohil et al., 2010), is now one of the most extensively studied medicinal plants for the treatment of various diseases, including cancer. As ongoing research uncovers new properties, it is becoming increasingly popular among scientists (Wiciński et al., 2024). The literature reports that extracts obtained from various parts of the CA plant using different solvents have demonstrated wound healing (Arribas-López et al., 2022), antioxidant (Jhansi & Kola, 2019), anticonvulsant (Deka et al., 2017), antiallergic, antipruritic, antiinflammatory (George & Joseph, 2009), antidiabetic (Rahman et al., 2012), antiulcer (Abdulla et al., 2010) and anticancer properties (Wiciński et al., 2024), both in vitro and in vivo. These properties of CA are due to various bioactive compounds such as triterpenes, carotenoids, glycosides, flavonoids and alkaloids (Razali et al., 2019). The main molecules responsible for its therapeutic properties are asiaticoside, asiatic acid, madecassoside and madecassic acid, which belong to the group of triterpenes (O. Bozkaya et al., 2023; Kandasamy et al., 2023). Asiatic acid has been identified as a possible anticancer medication or adjuvant therapeutic agent among these compounds (Wiciński et al., 2024). Asiatic acid has been demonstrated to suppress phosphorylation, induce cell death, and diminish tumor development and metastasis by influencing critical signaling pathways, including PI3K, Akt, mTOR, p70S6K, and STAT3 in cancer cells (Hao et al., 2018; Pang et al., 2024; Pantia et al., 2023; Zulkipli et al., 2020). The significance of acetic acid in diminishing the expression of indicators such as N-cadherin, β-catenin, claudin-1, and vimentin is noteworthy (Pantia et al., 2023). Research indicates that asiatic acid may induce autophagy in cancer cells by modulating the amounts of specific proteins, including LC3 and p62 (Pang et al., 2024). It may function as an anti-tumor immunotherapeutic drug due to its inductive action on Smad7 in conjunction with naringenin, a Smad3 inhibitor (Lian et al., 2018). Multiple in vitro and in vivo studies have demonstrated that acetic acid possesses potential anticancer characteristics that merit further examination in future research.

Alongside plant extracts, silver nanoparticles (AgNPs) functionalized with bioactive compounds have garnered significant attention in recent years as anticancer/antineoplastic agents for cancer detection and treatment applications (Ekici et al., 2023; Ekici et al., 2024). The pharmacological effect of AgNPs depends on various factors such as particle size, shape, surface charge, morphology, stability, dissolution rate, ion release ability, coating agent and the type of cell they interact with (Carlson et al., 2008; Jo et al., 2015). In addition to all these factors, the dose/concentration of AgNPs plays an important role in their therapeutic and cytotoxic effects (O. Bozkaya et

al., 2023). Hence, the physicochemical properties of AgNPs can affect cellular uptake, biodistribution, ability to penetrate biological barriers, as well as enhance the bioavailability of therapeutic compounds following both systemic and localized administration (Duan & Li, 2013).

In this study, the anticancer/antineoplastic properties of functional AgNPs synthesized via the green synthesis method were evaluated in vitro against SK-MEL-30 skin cancer, MCF-7 breast cancer, and H1299 lung cancer cell lines. The synthesis aimed to integrate the therapeutic properties of *Centella asiatica* extract with the controlled toxic effects of AgNPs.

## **Symbols and Abbreviations**

AgNPs	Silver Nanoparticles
CA	Centella asiatica

CA/AgNPs Centella asiatica/ Silver nanoparticles
IARC International Agency for Research on Cancer
LC3 Microtubule-associated protein 1A/1B-light chain 3

mTORC Mechanistic target of rapamycin complex

PI3K Phosphoinositide 3-kinases

STAT3 Signal transducer and activator of transcription 3

AgNO<sub>3</sub> Silver Nitrate NaOH Sodium hydoxide

MTT 3-(4,5-dimethylthiazol-2-yl)-2,5-diphenyltetrazolium bromide

°C Degree Celsius
PI Propodium iodide
MCF-7 Breast cancer
H1299 Lung cancer
SK-MEL-30 Skin Cancer

L929 Fibroblast

SPR Surface Plasmon Resonance

ZP Zeta Potential

DLS
SEM
Scanning Electron Microscopy
EDS
Energy Dispersive Spectroscopy
4',6-diamidino-2-phenylindole
FITC
Fluorescein isothiocyanate

## 2. Materials and methods

## 2.1. Materials

In this study, dried *Centella asiatica* leaves of Indian origin, procured from an authorized distributor in Turkey, were used. A 0.1 N AgNO<sub>3</sub> stock solution was purchased from Sigma-Aldrich (Germany). For the cytotoxicity assay, cell culture reagents, including DMEM, FBS, Trypsin/EDTA solution, and Penicillin/Streptomycin, were obtained from Biochrom (Merck, Germany), while other cell culture materials were sourced from Greiner (Austria). The cell culture experiments were conducted at the accredited in vitro biocompatibility laboratory within the Kırıkkale University Scientific and Technological Researches Application and Research Center (KÜBTUAM).

## 2.2. Preparation of CA extract

Approximately 5 grams of dried *Centella asiatica* leaves were extracted in a 50 mL methanol/water mixture (10:90% v/v) using a rotary extraction device at 40°C and 200 mbar pressure for 1 hour. Following the extraction, the mixture was filtered, and the solvent was removed using a rotary evaporator. The obtained solid extract was dissolved in water to prepare a stock solution with a final concentration of 1.0 M. The prepared solution was stored at +4°C for further experimental use.

#### 2.3. Synthesis of CA/AgNPs

A 1.0 M CA extract was filtered through a 0.45  $\mu$ m filter and transferred into a 20 mL Erlenmeyer flask. The solution was made basic by adding NaOH, after which AgNO<sub>3</sub> was added to achieve a final concentration of 1.0 mM, and the mixture was stirred. The solution was stirred at room temperature until the color changed from yellow to brown, and once it became stable, the stirring was stopped. The synthesized CA/AgNPs were then purified by passing through a 0.45  $\mu$ m filter and stored at +4 °C in Falcon tubes for preservation. The whole synthesis process is schematized in Figure 1.

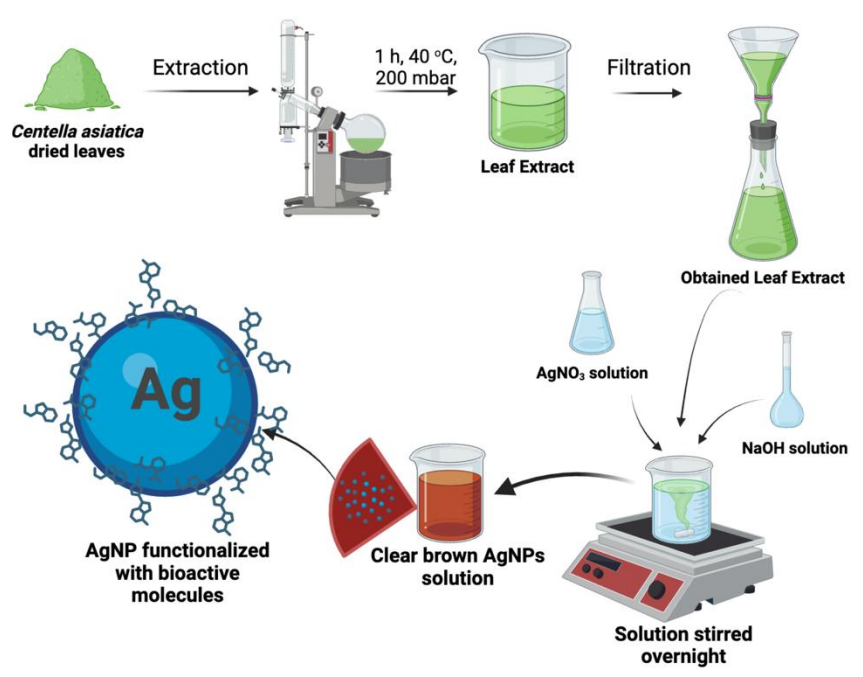


Figure 1. Schematic illustration of the synthesis steps of CA/AgNPs.

## 2.4. Characterization of CA/AgNPs

## 2.4.1. Ultraviyole-Visible (UV-Vis) spectrophotometer

The formation of CA/AgNPs was characterized using a UV-Vis spectrophotometer (Lambda 35, Perkin Elmer, USA) in the wavelength range of 350–500 nm.

#### 2.4.2. Zeta analysis

The average hydrodynamic diameters and zeta potential values of CA/AgNPs were determined using a Zeta-Sizer device (Nano ZS, Malvern Instruments, Malvern-UK).

## 2.4.3. Scanning electron microscope- Energy Dispersive Spectrometer (SEM-EDS) analysis

The morphology (particle size and shape) of the synthesized CA/AgNPs was characterized by field emission scanning electron microscopy (FE-SEM; Quanta FEG 250, FEI, Germany) operated at an accelerating voltage of 30 kV. Elemental analysis of silver was performed using energy dispersive X-ray spectroscopy (EDS; Octane Pro, AMETEK) integrated with the SEM; spectra were acquired at 30 kV with a magnification of approximately  $4.0 \times 10^4$ , a live time of 30 s, and a detector energy resolution of ~140 eV. Prior to analysis, CA/AgNPs dispersions were lyophilized; the resulting powders were mounted on aluminum stubs using carbon adhesive tape and sputter-coated with a thin Au/Pd layer to mitigate charging during imaging.

#### 2.5. Evaluation of cytotoxic and antineoplastic effects

The cytotoxic effects of 1.0 mM CA/AgNPs and CA extract were assessed using the 3-(4,5-dimethylthiazol-2-yl)-2,5-diphenyltetrazolium bromide (MTT) assay, following the previously described protocol (E. Bozkaya et al., 2023; O. Bozkaya et al., 2023; Bozkaya, Günay, et al., 2024; Sinmez et al., 2024). Human SK-MEL-30 skin cancer, MCF-7 breast cancer, H1299 lung cancer, and L929 fibroblast cells were seeded into 96-well plates at a density of 1×10<sup>4</sup> cells per well and incubated at 37 °C in a 5% CO<sub>2</sub>

atmosphere for 24 hours. After the incubation, cells were treated with serial dilutions (1:2, 1:4, 1:8, 1:16, 1:32, and 1:64) of 1.0 mM CA-AgNPs and CA extract, with the highest concentration adjusted to a 1:2 ratio using sterile medium. After 24 hours of treatment, the media were carefully removed and  $50\,\mu\text{L}$  of MTT solution (1 mg/mL) was added to each well. The plates were incubated for 2 hours at 37 °C. Following incubation,  $100\,\mu\text{L}$  of isopropanol was added to each well to dissolve the formazan crystals, and the absorbance was measured at 570 nm using a microplate reader.

To assess apoptotic and necrotic effects, MCF-7, H1299, SK-MEL-30, and L929 cell lines were seeded into 48-well plates at a density of  $2\times10^4$  cells per well. After 24 hours of incubation at 37 °C in a 5% CO<sub>2</sub> environment, cells were treated with the same dilution series (1:2 to 1:64) of 1.0 mM CA/AgNPs and CA extract. The treatments were incubated for an additional 24 hours under the same conditions. At the end of the treatment period, the culture media were discarded, and cells were stained with 100  $\mu$ L of a double-staining solution containing Hoechst 33342 and PI, both of which are DNA-binding fluorescent dyes. After 15 minutes of staining at room temperature in the dark, apoptotic and necrotic cells were examined using an inverted fluorescence microscope equipped with DAPI-FITC filters (excitation/emission: 480–520 nm), and the apoptotic and necrotic indices were calculated by expressing the number of apoptotic and necrotic cells as a ratio of the total cell count (Bozkaya, Bozkaya, et al., 2024; Dalkılıç et al., 2025; Rzayev et al., 2012).

## 3. Result and Discussion

## 3.1. Evaluation of CA/AgNPs by UV-Vis spectrometry

UV-Vis spectroscopy is a reliable and widely used technique for confirming the synthesis of AgNPs. In this study, the UV-Vis spectra of CA extract and CA/AgNPs solutions within the 300-700 nm wavelength range are presented in Figure 2a. According to the literature, the absorption bands of AgNPs typically appear within the 390-500 nm range, while the peak positions vary between 400-450 nm, depending on parameters such as particle size, shape, temperature, capping agent, and pH (Begum et al., 2018; Fernando & Zhou, 2019). While the CA extract does not exhibit a distinct peak in this range, the CA/AgNPs solution displays an absorption peak at a maximum wavelength of 415 nm. This finding confirms that AgNPs have been successfully synthesized using CA extract. Moreover, the obtained results are in good agreement with the characteristic data of AgNPs synthesized via plant extracts, as reported in the literature (O. Bozkaya et al., 2023; Ekici et al., 2023; Ekici et al., 2024). Additionally, the color change of the solution from yellow-green to translucent brown after the reaction serves as further visual evidence of AgNP formation (Figure 2b) (O. Bozkaya et al., 2023; Gün Gök et al., 2020).

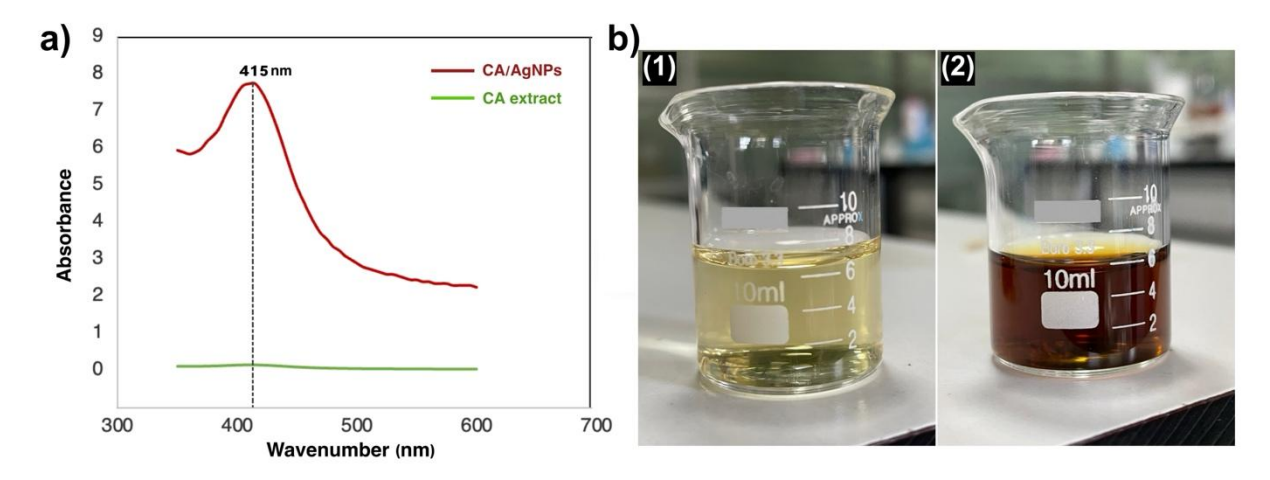


Figure 2. (a) UV-Vis spectrum of CA extract and CA/AgNPs solutions; (b1) CA extract solution); (b2) CA/AgNPs solution.

## 3.2. Evaluation of the stability of CA/AgNPs by Zeta analysis

Zeta potential is a crucial parameter in colloidal systems, determining the electrostatic stability and surface charge of nanoparticles. It represents the potential difference between the electrical double layer surrounding a nanoparticle and the bulk solution, influencing dispersion stability and aggregation tendencies (Pochapski et al., 2021). A high absolute zeta potential value (typically  $> \pm 30$  mV) indicates strong electrostatic repulsion, enhancing colloidal stability, while lower values suggest a tendency for particle aggregation (Németh et al., 2022). In biomedical applications, particularly in cell culture systems, the zeta potential affects cellular uptake, protein corona formation, and interaction with biomolecules, thereby influencing nanoparticle cytotoxicity, biocompatibility, and overall efficacy (Moraru et al., 2020). In this study, the zeta potential (ZP) of the synthesized CA/AgNPs were measured as -21.3 mV  $\pm$  3.60 mV (Figure 3a). The determined ZP value and a single sharp dispersion peak indicate moderate colloidal stability. A ZP within the

range of -20 to -30 mV suggests that the system possesses a certain degree of stability; however, it may also carry a risk of aggregation in long-term studies. Although a ZP greater than  $\pm 30$  mV is considered ideal for high stability, the obtained value is still sufficient to maintain dispersion in a cell culture environment. The hydrodynamic diameters of CA/AgNPs were analyzed by dynamic light scattering (DLS) method with the same device and the size distribution curve is shown in Figure 3b. The mean hydrodynamic size of CA/AgNPs was determined to be 29.77 nm (PdI < 0.7). This This size distribution places the nanoparticles within the optimal range for cellular internalization, as nanoparticles between 10-100 nm have demonstrated efficient uptake via endocytosis and passive diffusion mechanisms (Hoshyar et al., 2016). AgNPs are well known for their antimicrobial and cytotoxic properties, which can vary based on their surface charge, size, and interaction with biological media (Albanese et al., 2012). Therefore, the observed size and zeta potantial supports penetration into cellular compartments, making CA/AgNPs a promising candidate for targeted biomedical applications, including cancer therapy, antimicrobial coatings, and controlled drug release systems.

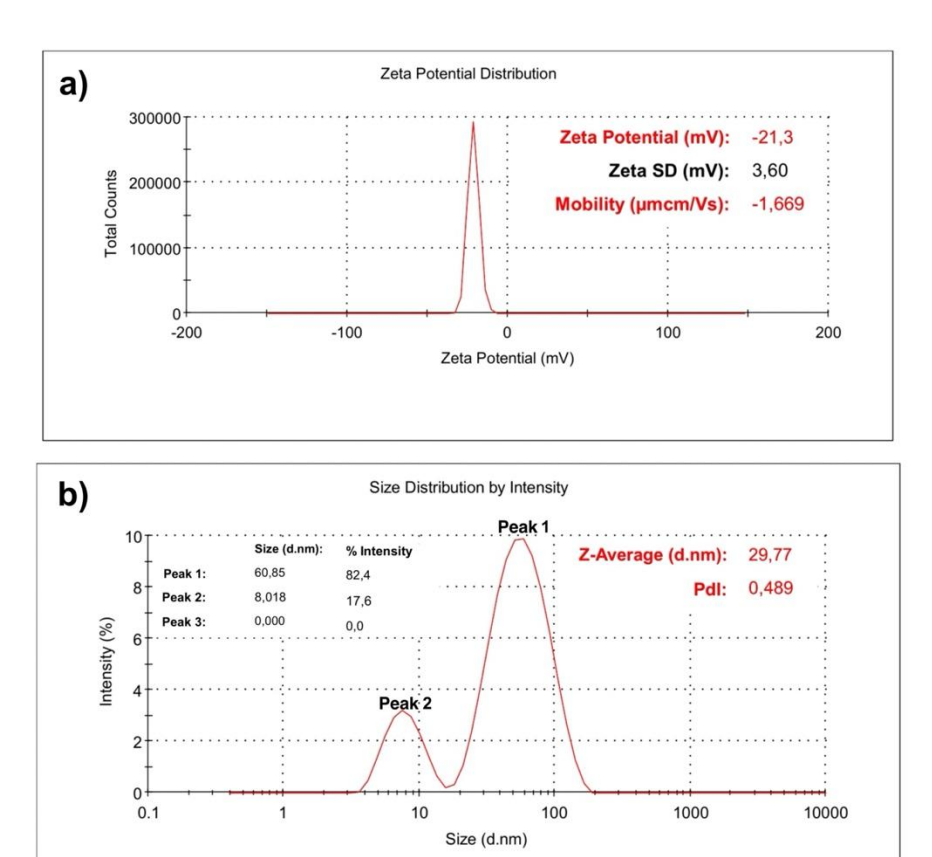


Figure 3. (a) Zeta potential distribution curve; (b) hydrodynamic size distribution curve of CA/AgNPs.

## 3.3. Morphological and elemental evaluation of CA/AgNPs

The morphology, shape, and size distribution of the synthesized CA/Ag NPs were examined using Scanning Electron Microscopy (SEM) (Figure 4). Due to the analysis conditions, the nanoparticles appeared in a grape-like arrangement (Figure 4a) yet predominantly exhibited a spherical shape (Figure 4b) with a relatively uniform distribution and a size below 100 nm (Figure 4c). Measurements from selected regions revealed an average particle size of approximately  $50\pm20$  nm, which is in reasonable agreement with the Zeta size distribution results.

Additionally, the elemental composition of the AgNPs was analyzed using Energy Dispersive Spectroscopy (EDS). As shown in Figure 4e, a sharp peak was observed at 3 keV, corresponding to the Lα energy band of silver (Ag), confirming the presence of Ag atoms in the synthesized nanoparticle structure (Gün Gök et al., 2021; Rauf et al., 2025). The size, shape and core composition of nanoparticles stand out as critical determinants in cellular uptake processes (Albanese et al., 2012; Hoshyar et al., 2016). Nanoparticles with different morphologies such as spherical, cubic, rod-like, or worm-like can have distinct effects on intracellular uptake mechanisms. In a study conducted by Gratton et al. (2008), rod-shaped nanoparticles demonstrated the highest cellular uptake among particles larger than 100 nm, followed by spherical, cylindrical, and cubic particles (Gratton et al., 2008). However, for nanoparticles smaller than 100 nm, research has shown that spherical nanoparticles exhibit higher cellular uptake efficiency compared to rod-shaped counterparts

(Chithrani et al., 2006; Qiu et al., 2010). Given these findings, the CA/AgNPs synthesized in this study, which are predominantly spherical and have an average size below 100 nm, are considered well-suited for effective cellular uptake.

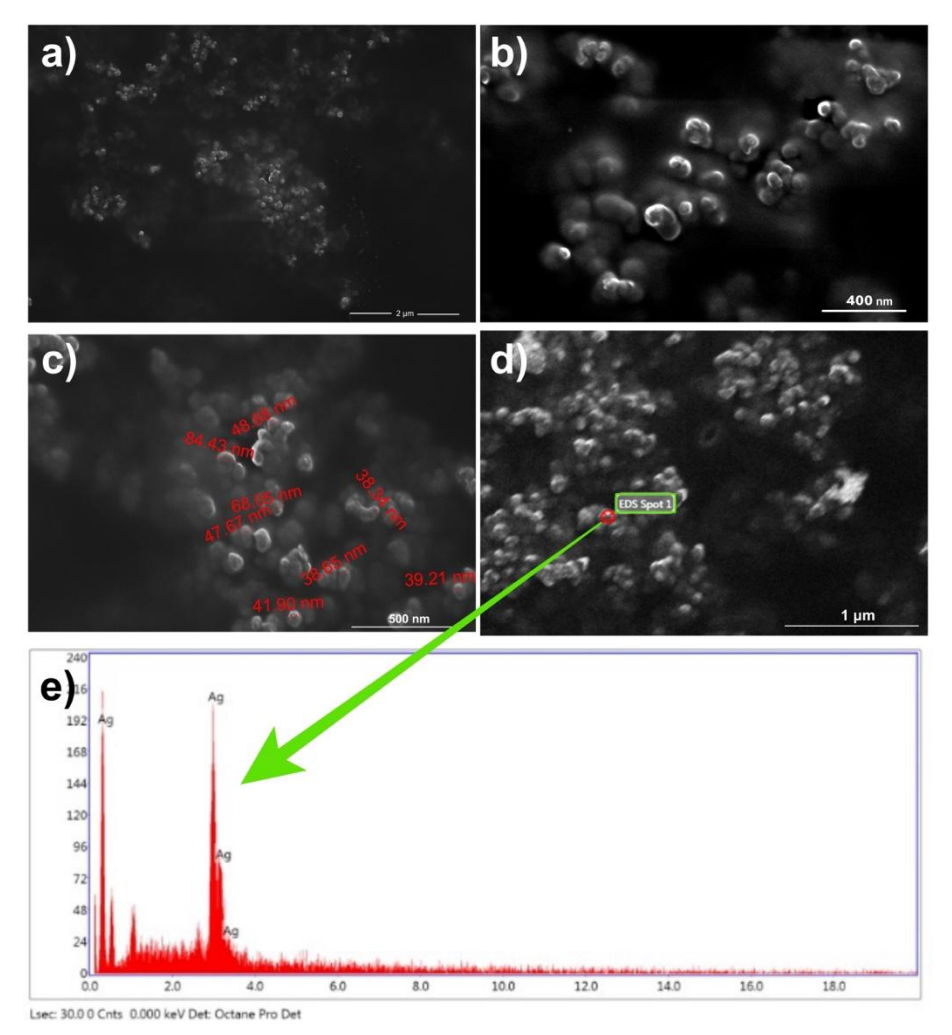


Figure 4. (a-d) SEM images; (e) EDS analysis spectrum of the synthesized CA/AgNPs.

#### 3.4. Assessment of antineoplastic/anticancer activity of CA/AgNPs

Materials with both antimicrobial and anticancer properties stand out as promising therapeutic candidates for immunocompromised cancer patients due to their ability to induce selective cytotoxicity and effectively reduce bacterial and fungal infections (Soyingbe et al., 2018). In a previous study (O. Bozkaya et al., 2023), the in vitro cytotoxicity and antimicrobial activity of CA/AgNPs at concentrations between 0.1 mM and 10 mM were systematically evaluated. MTT assay results showed that concentrations above 1 mM decreased cell viability below 70% and produced significant cytotoxic effects. Therefore, the highest concentration of 1 mM CA/AgNPs solution was determined, which exhibited both no cytotoxic effect and effective antimicrobial activity. Based on these findings, this concentration was chosen in the present study to evaluate its potential in anticancer applications. Furthermore, the plant extract used in the synthesis has been previously shown in the literature to exhibit pronounced anticancer properties (Rai et al., 2014).

The effects of AgNPs synthesized with CA extract on cell viability were investigated in H1299 lung cancer, MCF-7 breast cancer, SK-MEL-30 skin cancer, and L929 fibroblast cell lines. As shown in Figure 5, cell viability was found to be dose-dependent across all tested cell lines. Specifically, in H1299 lung cancer cells, treatment with both CA extract and CA-AgNPs at a 1/2 dilution exhibited pronounced cytotoxic effects, with viability dropping below 50%. At a 1/4 dilution, the highest viability was observed in cells treated with CA extract, calculated at  $53.8 \pm 0.8\%$ . A gradual increase in cell viability was noted with decreasing concentrations, reaching a maximum of  $84.1 \pm 0.6\%$  at the lowest dilution (1/64) in cells treated with 1 mM CA-AgNPs synthesized using 5 mL of CA extract. In MCF-7 breast cancer cells, the lowest viability ( $50.7 \pm 0.6\%$ ) was observed at higher concentrations in cells treated with CA extract. At 1/4 dilution, the highest viability was recorded as  $72.9 \pm 0.5\%$  in cells treated with 1 mM CA-AgNPs. Similar to H1299 cells, a clear dose-dependent increase in cell viability was observed, with the maximum viability reaching  $91.9 \pm 1.5\%$  at the lowest

concentration (1/64) of 1 mM CA-AgNPs. In the case of SK-MEL-30 skin cancer cells, CA extract exhibited cytotoxicity at all applied concentrations, with the lowest viability of  $33.3 \pm 0.4\%$  observed at the highest concentration. However, a concentration-dependent increase in viability was observed in cells treated with 1 mM CA-AgNPs synthesized using 5 mL of CA extract. Compared to the other cell lines, SK-MEL-30 skin cancer cells were observed to be highly sensitive to both CA extract and CA/AgNPs treatment. This difference may be attributed to variations in cellular structure, morphology, surface chemistry, and intracellular mechanisms. SK-MEL-30 is an adherent, epithelial-like melanoma cell line carrying the NRAS Q61K mutation, which renders the cells more dependent on proliferative signaling and increases their susceptibility to oxidative stress (Cellosaurus: CVCL 0039). Melanoma cells are also known to express high levels of MHC class I antigens and other surface glycoproteins, potentially facilitating nanoparticle uptake and enhancing the intracellular delivery of CA/AgNPs (Diaz et al., 2023; Himalini et al., 2022). Furthermore, the triterpenes of Centella asiatica (e.g., asiaticoside and madecassoside) have been shown to induce cell cycle arrest, DNA damage, and apoptosis in different cancer cell types, and in melanoma cells they may trigger programmed cell death via p53 dependent and independent pathways, including caspase-3 activation (Hao et al., 2018; Lian et al., 2018; Pang et al., 2024; Pantia et al., 2023; Zulkipli et al., 2020). On the other hand, the cytotoxic effect of AgNPs is largely mediated by the induction of reactive oxygen species (ROS), lipid peroxidation, and mitochondrial dysfunction. Given the already elevated basal ROS levels in melanoma cells, AgNP exposure may synergistically amplify oxidative stress, resulting in more pronounced cytotoxicity (Zhang et al., 2014). For L929 fibroblast cells, the highest cell viability at the highest concentration was  $72.4 \pm 0.6\%$  in cells treated with 1 mM CA-AgNPs, while CA extract-treated cells showed a slightly lower viability of  $68.3 \pm 1.2\%$ . At lower concentrations, both CA extract and CA-AgNPs demonstrated increased cell viability, with maximum values of  $99.2 \pm 1.5\%$  and  $89.1 \pm 2.0\%$ , respectively, at a 1/64 dilution.

Overall, the MTT assay results show that CA/AgNPs did not show any cytotoxic effect on normal L929 fibroblast cells even at the highest concentrations tested, whereas a significant cytotoxic effect was observed in all cancer cell lines tested. These findings are in agreement with the literature that AgNPs may exhibit selective toxicity against cancer cells.

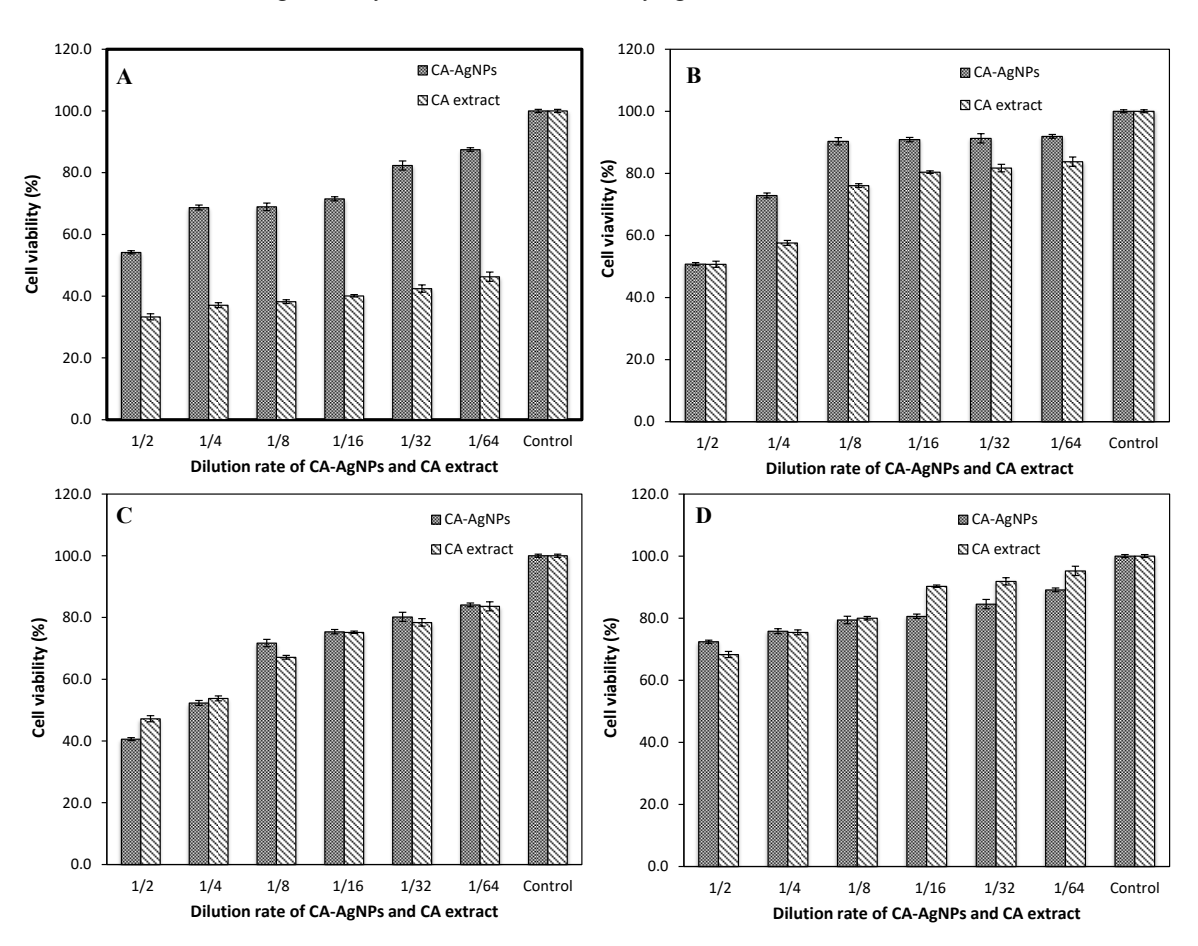


**Figure 4.** MTT test results showing cell viability performed with **(a)** SK-MEL-30 skin cancer; **(b)** MCF-7 breast cancer; **(c)** H1299 lung cancer; **(d)** L929 fibroblast cells.

In the double-staining method, apoptotic cells appear bright blue under the DAPI filter, while necrotic cells are visualized in red under the FITC filter. The key distinction between apoptotic and necrotic nuclei lies in the occurrence of DNA fragmentation and chromatin condensation during apoptosis, which is absent in necrosis. Necrosis is characterized instead by a loss of membrane integrity and

cellular swelling (E. Bozkaya et al., 2023; Melekoğlu et al., 2020). Based on the apoptotic and necrotic evaluation of SK-MEL-30 skin cancer, MCF-7 breast cancer, H1299 lung cancer, and L929 fibroblast cells as observed under fluorescence microscopy (images presented in Figure 5) cells undergoing apoptosis or necrosis were identified through morphological markers such as karyorrhexis (nuclear fragmentationn) and pyknosis (chromatin condensation) (Akturk, 2020; Bozkaya, Bozkaya, et al., 2024). Quantitative results regarding the apoptotic and necrotic indices of each cell line are summarized in Table 1 and Table 2, respectively.

According to the apoptotic index results, the highest rate of apoptosis at the 1/2 concentration was observed in H1299 lung cancer cells. In this group, the apoptotic index was calculated as  $25.3 \pm 2.3\%$  in cells treated with CA extract, while it was  $15 \pm 2.4\%$  in cells exposed to CA-AgNPs. At the lowest concentration (1/64), the apoptotic index decreased to  $5.6 \pm 1.2\%$  for CA extract and  $4.4 \pm 1.8\%$  for CA-AgNP-treated H1299 cells, indicating a clear dose-dependent reduction in apoptosis. These results are in line with previous studies demonstrating the pro-apoptotic effect of CA phytochemicals on lung cancer cells. In particular, asiaticoside, a major component of CA, has been shown to induce apoptosis in A549 lung cancer cells via the mitochondrial pathway, suggesting that CA-derived compounds can act as effective anti-cancer agents (Wu et al., 2017). In SK-MEL-30 skin cancer cells, the apoptotic indices at the 1/2 concentration were determined to be  $19 \pm 1.5\%$  for CA extract and  $9 \pm 0.4\%$  for CA-AgNPs. Interestingly, at the 1/64 dilution, the CA extract group maintained a relatively high apoptotic index of  $11.7 \pm 0.6\%$ , representing the highest apoptosis rate observed at low concentration across all cell lines tested. The ability of CA extract to induce apoptosis in melanoma cells is consistent with findings by, Hsu et al. who reported that CA exerts apoptotic effects in skin cancer models through modulation of oxidative stress and caspase activation. This sustained apoptotic effect even at low concentrations suggests a potent cytotoxic mechanism that warrants further exploration in melanoma therapy (Hsu et al., 2005). For MCF-7 breast cancer cells, the apoptotic indices at the 1/2 concentration were 17±1.5% for CA extract and 9±0.4% for CA-AgNPs. Similar to other cell lines, a decrease in CA extract and CA-AgNPs concentration resulted in a corresponding reduction in apoptotic activity. These findings are strongly supported by the work of Fard et al. (2018), who demonstrated that silver nanoparticles biosynthesized using CA leaf extract induce dose-dependent apoptosis in MCF-7 cells via caspase-3 and caspase-9 activation (Fard et al., 2018). The observed reduction in apoptosis at lower doses aligns with typical concentration-response behavior seen in phytochemical-based cancer therapeutics.

According to the necrotic index results, the necrotic index was  $38.5\pm1\%$  in SK-MEL-30 cells that treated with CA extract at 1/2 concentration and the highest toxicity was determined in that cell line. The necrotic index of SK-MEL-30 cells that treated with CA/AgNPs at the same concentration was calculated as  $25.5\pm1.2\%$ . The necrotic index was  $37.3\pm1.2\%$  and  $37.5\pm0.8$ , respectively, in MCF-7 cells to which CA/AgNPs and CA extract were applied at 1/2 concentration, and a decrease in toxicity was observed as the concentration decreased. It was observed that toxicity was high at high concentrations in H1299 cells, and the necrotic index decreased significantly after 1/8 concentration. In L929 fibroblast cells, it is seen that the necrotic index is low and there is no significant toxicity. Both apoptotic and necrotic index results support the MTT test results for SK-MEL-30 skin cancer, MCF-7 breast cancer, H1299 lung cancer and L929 fibroblast cells.

Table 1. The apoptotic index results of SK-MEL-30 skin cancer, MCF-7 breast cancer, H1299 lung cancer and L929 fibroblast cells.

Cell lines	Sample	Dilution rate of CA-AgNPs and CA extract					
		1/2	1/4	1/8	1/16	1/32	1/64
SK-MEL-30	CA/AgNPs	9±0.4	8.2±0.2	8±0.6	7.5±0.7	5±0.8	3±0.8
	CA extract	19±1.5	18.5±0.6	15.4±1.4	14±2.2	12.5±0.8	11.7±0.6
MCF-7	CA/AgNPs	9±0.4	8.5±0.5	7.2±0.2	7±0.3	5.4±0.7	3±0.5
	CA extract	17±1.5	15.6±1	14.2±0.6	13±1.3	12.6±1.5	9±1
Н1299	CA/AgNPs	15±2.4	13.5±3.4	10±1.2	8.5±1.5	5.6±2.8	4.4±1.8
	CA extract	25.3±2.3	22.1±0.7	16.4±0.6	12.1±1.8	8.2±0.6	5.6±1.2
L929	CA/AgNPs	10±0.5	9.5±0.8	7.5±0.3	6±0.7	5.5±0.8	5.2±0.7
	CA extract	7.2±1.3	5.4±0.6	5±0.8	5±0.5	3.5±1.2	3±0.6

Table 2. The necrotic index results of SK-MEL-30 skin cancer, MCF-7 breast cancer, H1299 lung cancer and L929 fibroblast cells.

Cell lines	Sample	Dilution rate of CA-AgNPs and CA extract					
		1/2	1/4	1/8	1/16	1/32	1/64
SK-MEL-30	CA-AgNPs	25.5±1.2	22.4±1	18.6±1.4	15±1.2	13.6±1.5	10.8±1.2
	CA extract	38.5±1	33.2±2.1	28.5±0.8	25.3±0.7	22.6±1	21.7±1.4
MCF-7	CA-AgNPs	37.3±1.2	25±0.8	12±0.6	9.5±1.4	7.5±0.5	6.8±0.8
	CA extract	37.5±0.8	27.4±2.3	22±0.2	20.5±1.7	18.4±0.4	15.2±0.2
H1299	CA-AgNPs	33.5±1.8	28.3±1.5	18.6±3.5	13.4±2.3	7.2±1.2	5.3±0.8
	CA extract	27.2±1.5	19.5±1.2	15.3±2.1	10.8±2.3	4,5±1	2.3±0.5
L929	CA-AgNPs	12±1.2	10.8±1	8.2±0.4	7.3±1.2	6.2±1.5	5±1.5
	CA extract	10.3±1	8.6±0.8	7.1±1	7±0.5	5±1.4	3.2±0.8

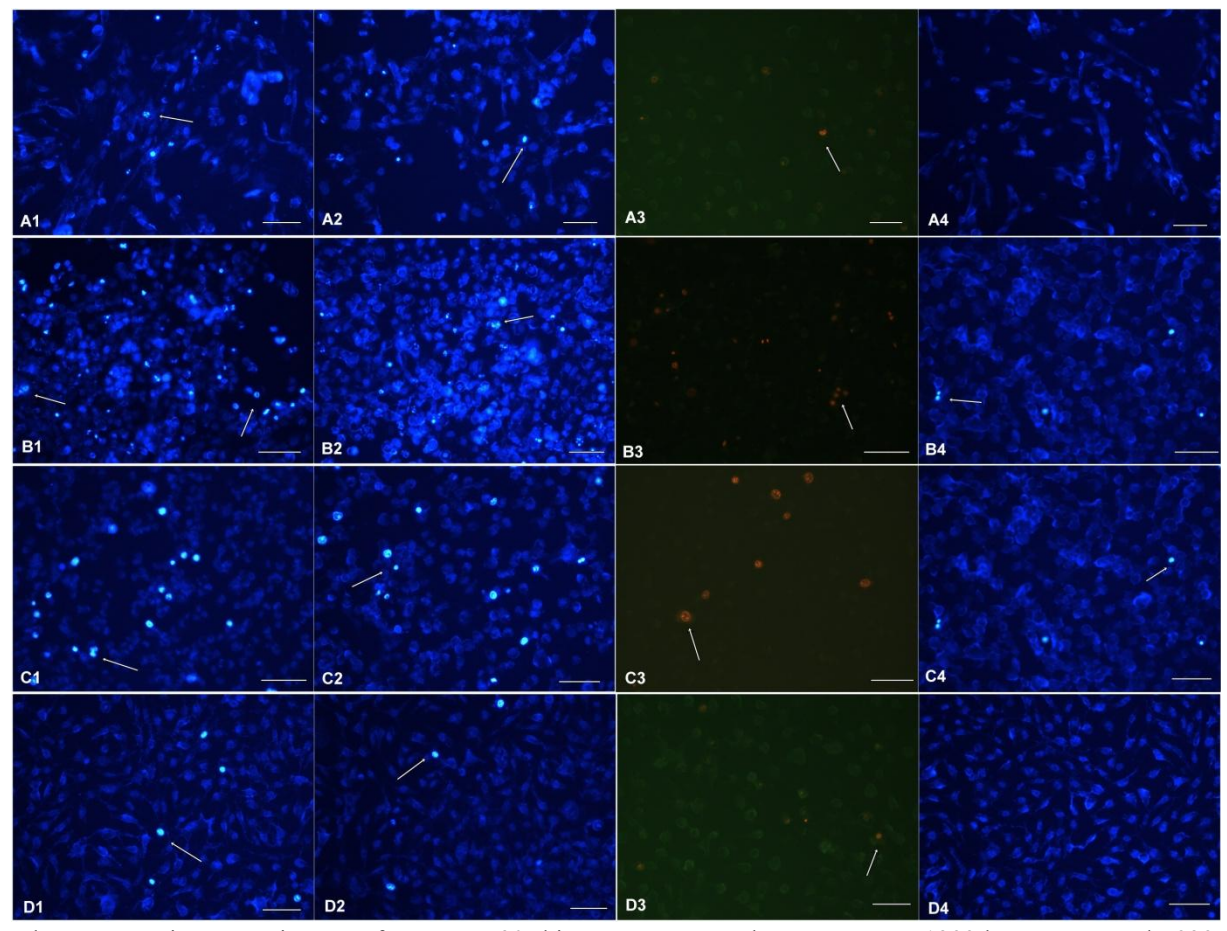


Figure 5. Fluorescent microscopy images of SK-MEL-30 skin cancer, MCF-7 breast cancer, H1299 lung cancer and L929 fibroblast cells that were cultured with CA/AgNPs and CA extract. (a) apoptotic necrotic index photographs of SK-MEL-30 skin cancer cell, the bar indicates 100 μm; (b1) apoptotic cells treated with 1/2 ratio of CA extract; (a2) apoptotic cells treated with 1/4 of CA/AgNPs; (a3) necrotic cells treated with 1/64 CA/AgNPs; (a4) control group cells; (b) apoptotic necrotic index photographs of MCF-7 breast cancer cell, the bar indicates 100 μm; (b1) apoptotic cells treated with 1/2 CA extract; (b2) apoptotic cells treated with 1/4 of CA/AgNPs; (b3) necrotic cells treated with 1/16 CA/AgNPs; (b4) control group cells; (c) Apoptotic necrotic index photographs of cell H1299 lung cancer cell, the bar indicates 100 μm; (c1) apoptotic cells treated with 1/2 of CA extract; (c2) apoptotic cells treated with 1/4 of CA-AgNPs; (c3) necrotic cells treated with 1/8 CA/AgNPs; (c4) control group cells; (d) Apoptotic necrotic index photographs of L929 fibroblast cell, the bar indicates 100 μm; (d1) apoptotic cells treated with 1/2 of CA extract; (d2) apoptotic cells treated with 1/4 of CA/AgNPs; (d3) necrotic cells treated with 1/16 CA/AgNPs; (d4) control group cells.

Overall, both apoptotic and necrotic index values correlate well with the MTT assay results, confirming the selective cytotoxic effects of CA and CA/AgNPs on cancerous cells (SK-MEL-30, MCF-7, H1299), while maintaining low toxicity in normal L929 fibroblast cells. These outcomes underline the therapeutic potential of *Centella asiatica*-based silver nanoparticles as effective and biocompatible anticancer agents.

## 4. Conclusion

This study revealed that *Centella asiatica* (CA) extract and CA-mediated silver nanoparticles (CA/AgNPs) exhibit significant and selective cytotoxic effects against H1299 lung cancer, MCF-7 breast cancer, and SK-MEL-30 skin cancer cell lines, while showing minimal toxicity toward normal L929 fibroblast cells. Apoptotic and necrotic index results were consistent with MTT assay findings and demonstrated a clear dose-dependent response across all cancer cell lines. In particular, the highest apoptotic index was observed in H1299 cells treated with CA extract, suggesting that phytochemicals such as asiaticoside present in C. asiatica may trigger apoptosis via mitochondrial pathways. Similarly, increased levels of apoptosis and necrosis were observed in SK-MEL-30 and MCF-7 cells, particularly at higher concentrations. The higher necrotic effect observed with CA extract alone compared to CA/AgNPs suggests that the nanoparticle formulation may provide a more controlled release of active compounds, thereby reducing non-specific cytotoxicity. In addition to cytotoxicity, the findings indicate that both CA and CA/AgNPs possess notable antineoplastic properties. Previous studies have shown that CA exerts multifaceted antitumor effects, including inhibition of tumor growth, suppression of angiogenesis, prevention of metastasis, and arrest of the cell cycle. Specifically, its active constituents have been reported to induce G1 or G2/M

phase arrest and activate apoptosis via caspase-3 and caspase-9 pathways. It is likely that the nanoparticle formulation further enhances these mechanisms by improving cellular uptake and increasing bioavailability at the target site. The low apoptotic and necrotic indices observed in L929 fibroblast cells also confirm the biocompatibility of both CA extract and CA/AgNPs, in line with the known tissue-regenerative and cytoprotective effects of *CA*. In conclusion, CA and its AgNP formulations demonstrate both cytotoxic and antineoplastic activity, making them promising candidates for targeted cancer therapy or combinational treatment strategies. However, further mechanistic studies and comprehensive in vivo evaluations are required to validate their therapeutic potential and ensure their safety in clinical applications.

## **Declaration of Competing Interest**

There are no conflicts to declare.

## Acknowledgement

The author is grateful to Kırıkkale University Scientific and Technological Research Application and Research Center for their support.

#### References

Abdulla, M., Al-Bayaty, F., Younis, L., & Abu Hassan, M. (2010). Anti-ulcer activity of Centella asiatica leaf extract against ethanol-induced gastric mucosal injury in rats. *Journal of medicinal plants research*, 4(13), 1253-1259.

Akturk, O. (2020). Colloidal stability and biological activity evaluation of microbial exopolysaccharide levan-capped gold nanoparticles. *Colloids and Surfaces B: Biointerfaces*, 192, 111061. https://doi.org/https://doi.org/10.1016/j.colsurfb.2020.111061

Albanese, A., Tang, P. S., & Chan, W. C. (2012). The effect of nanoparticle size, shape, and surface chemistry on biological systems. *Annual Review of Biomedical Engineering*, 14(1), 1-16.

Arribas-López, E., Zand, N., Ojo, O., Snowden, M. J., & Kochhar, T. (2022). A systematic review of the effect of Centella asiatica on wound healing. *International Journal of Environmental Research and Public Health*, 19(6), 3266.

Begum, R., Farooqi, Z. H., Naseem, K., Ali, F., Batool, M., Xiao, J., & Irfan, A. (2018). Applications of UV/Vis spectroscopy in characterization and catalytic activity of noble metal nanoparticles fabricated in responsive polymer microgels: a review. *Critical Reviews in Analytical Chemistry*, 48(6), 503-516.

Bozkaya, E., Türk, M., Ekici, H., & Karahan, S. (2023). Investigation of the biocompatibility and in vivo wound healing effect of Cotinus coggygria extracts. *Ankara Üniversitesi Veteriner Fakültesi Dergisi*, 1-12. <a href="https://doi.org/10.33988/auvfd.1217177">https://doi.org/10.33988/auvfd.1217177</a>

Bozkaya, O., Bozkaya, E., Ekici, H., Alçığır, M. E., Şahin, Y., Aytuna Çerçi, N., Karahan, S., Yiğitoğlu, M., & Vargel, İ. (2024). Evaluation of Burn Wound Healing Efficacy and Biocompatibility of Centella asiatica Mediated Synthesised AgNPs Loaded Hybrid Nanofiber Scaffold: In Vitro and In Vivo Studies. *Macromolecular Materials and Engineering*, 309(12), 2400186. <a href="https://doi.org/10.1002/mame.202400186">https://doi.org/10.1002/mame.202400186</a>

Bozkaya, O., Ekici, H., GÜN GÖK, Z., Bozkaya, E., Ekici, S., Yiğitoğlu, M., & Vargel, İ. (2023). Investigation of the in vitro antibacterial, cytotoxic and in vivo analgesic effects of silver nanoparticles coated with Centella asiatica plant extract. *Ankara Üniversitesi Veteriner Fakültesi Dergisi*, 70(1), 87-96. <a href="https://doi.org/https://doi.org/10.33988/auvfd.1014802">https://doi.org/https://doi.org/https://doi.org/10.33988/auvfd.1014802</a>

Bozkaya, O., Günay, K., Bozkaya, E., & Arslan, M. (2024). Poly (hexamethylene biguanide) immobilized non-absorbable and antimicrobial PET fiber for surgical suture applications: synthesis, characterization and in vitro cytocompatibility assessment. *International Journal of Engineering Research and Development*, 16(2), 778-791.

Carlson, C., Hussain, S. M., Schrand, A. M., K. Braydich-Stolle, L., Hess, K. L., Jones, R. L., & Schlager, J. J. (2008). Unique cellular interaction of silver nanoparticles: size-dependent generation of reactive oxygen species. *The journal of physical chemistry B*, 112(43), 13608-13619.

Chithrani, B. D., Ghazani, A. A., & Chan, W. C. (2006). Determining the size and shape dependence of gold nanoparticle uptake into mammalian cells. *Nano Letters*, 6(4), 662-668.

Cohen, I. S., Mosher, M. B., O'Keefe, E. J., Klaus, S. N., & De Conti, R. C. (1973). Cutaneous toxicity of bleomycin therapy. *Archives of Dermatology*, 107(4), 553-555.

- Dalkılıç, S., Kadıoğlu Dalkılıç, L., İsbenov, E., Uygur, L., & Taşdemir, C. (2025). Investigation of Cytotoxic, Antioxidant, Apoptotic/Necrotic Activity of Aquilaria agallocha Root Extract and Determination of Gene Expression Levels in HepG2, MCF-7 Cancer Cell Lines. *Life*, 15(4), 651.
- Deka, D., Chakravarty, P., & Purkayastha, A. (2017). Evaluation of the anticonvulsant effect of aqueous extract of centella asiatica in albino mice. *Int J Pharm Pharm Sci*, 9(2), 312-314.
- Desai, A. G., Qazi, G. N., Ganju, R. K., El-Tamer, M., Singh, J., Saxena, A. K., Bedi, Y. S., Taneja, S. C., & Bhat, H. K. (2008). Medicinal plants and cancer chemoprevention. *Current Drug Metabolism*, 9(7), 581-591. <a href="https://doi.org/10.2174/138920008785821657">https://doi.org/10.2174/138920008785821657</a>
- Diaz, M. J., Natarelli, N., Aflatooni, S., Aleman, S. J., Neelam, S., Tran, J. T., Taneja, K., Lucke-Wold, B., & Forouzandeh, M. (2023). Nanoparticle-Based Treatment Approaches for Skin Cancer: A Systematic Review. *Current Oncology (Toronto, Ont.)*, 30(8), 7112-7131. <a href="https://doi.org/10.3390/curroncol30080516">https://doi.org/10.3390/curroncol30080516</a>
- Duan, X., & Li, Y. (2013). Physicochemical characteristics of nanoparticles affect circulation, biodistribution, cellular internalization, and trafficking. *Small*, 9(9-10), 1521-1532.
- Ekici, S., Bozkaya, E., Bozkaya, O., Cerci, N. A., Aluc, Y., & Ekici, H. (2023). Vitex Agnus-Castus L. Nanoparticles: Preparation, Characterization and Assessment of Antimicrobial and Anticancer Activity. *ChemistrySelect*, 8(32), e202302102. <a href="https://doi.org/10.1002/slct.202302102">https://doi.org/10.1002/slct.202302102</a>
- Ekici, S., Bozkaya, O., Sevin, S., Erdem, B., Arslan, O. C., Özgenç Cinar, O., Bozkaya, E., & Ekici, H. (2024). Investigation of the biological activity and toxicity of bioactive silver nanoparticles synthesized via Vitex agnus-castus seed extract on honey bees. *Veterinary Research Communications*, 48(6), 3813-3821.
- Fard, S. E., Tafvizi, F., & Torbati, M. B. (2018). Silver nanoparticles biosynthesised using Centella asiatica leaf extract: apoptosis induction in MCF-7 breast cancer cell line. *IET Nanobiotechnology*, 12(7), 994-1002. <a href="https://doi.org/https://doi.org/10.1049/iet-nbt.2018.5069">https://doi.org/https://doi.org/10.1049/iet-nbt.2018.5069</a>
- Fernando, I., & Zhou, Y. (2019). Impact of pH on the stability, dissolution and aggregation kinetics of silver nanoparticles. *Chemosphere*, 216, 297-305.
- George, M., & Joseph, L. (2009). Anti-allergic, anti-pruritic, and anti-inflammatory activities of Centella asiatica extracts. *African Journal of Traditional, Complementary and Alternative Medicines*, 6(4).
- Gibaud, S., Andreux, J., Weingarten, C., Renard, M., & Couvreur, P. (1994). Increased bone marrow toxicity of doxorubicin bound to nanoparticles. *European Journal of Cancer*, 30(6), 820-826.
- Gohil, K. J., Patel, J. A., & Gajjar, A. K. (2010). Pharmacological review on Centella asiatica: a potential herbal cure-all. *Indian Journal of Pharmaceutical Sciences*, 72(5), 546.
- Graham, J., Quinn, M., Fabricant, D., & Farnsworth, N. (2000). Plants used against cancer—an extension of the work of Jonathan Hartwell. *Journal of Ethnopharmacology*, 73(3), 347-377.
- Gratton, S. E., Ropp, P. A., Pohlhaus, P. D., Luft, J. C., Madden, V. J., Napier, M. E., & DeSimone, J. M. (2008). The effect of particle design on cellular internalization pathways. *Proceedings of the National Academy of Sciences of the United States of America*, 105(33), 11613-11618. <a href="https://doi.org/10.1073/pnas.0801763105">https://doi.org/10.1073/pnas.0801763105</a>
- Gün Gök, Z., Günay, K., Arslan, M., Yiğitoğlu, M., & Vargel, İ. (2020). Coating of modified poly (ethylene terephthalate) fibers with sericin-capped silver nanoparticles for antimicrobial application. *Polymer Bulletin*, 77(4), 1649-1665.
- Gün Gök, Z., Yiğitoğlu, M., Vargel, İ., Şahin, Y., & Alçığır, M. E. (2021). Synthesis, characterization and wound healing ability of PET based nanofiber dressing material coated with silk sericin capped-silver nanoparticles. *Materials Chemistry and Physics*, 259, 124043. https://doi.org/10.1016/j.matchemphys.2020.124043
- Hao, Y., Huang, J., Ma, Y., Chen, W., Fan, Q., Sun, X., Shao, M., & Cai, H. (2018). Asiatic acid inhibits proliferation, migration and induces apoptosis by regulating Pdcd4 via the PI3K/Akt/mTOR/p70S6K signaling pathway in human colon carcinoma cells. *Oncology Letters*, 15(6), 8223-8230.

Himalini, S., Nallal, V. U. M., Razia, M., Chinnapan, S., Chandrasekaran, M., Ranganathan, V., Gatasheh, M. K., Hatamleh, A. A., Al-Khattaf, F. S., & Kanimozhi, S. (2022). Antimicrobial, anti-melanogenesis and anti-tyrosinase potential of myco-synthesized silver nanoparticles on human skin melanoma SK-MEL-3 cells. *Journal of King Saud University-Science*, 34(3), 101882.

Hoshyar, N., Gray, S., Han, H., & Bao, G. (2016). The effect of nanoparticle size on in vivo pharmacokinetics and cellular interaction. *Nanomedicine (Lond)*, 11(6), 673-692. https://doi.org/10.2217/nnm.16.5

Hsu, Y.-L., Kuo, P.-L., Lin, L.-T., & Lin, C.-C. (2005). Asiatic acid, a triterpene, induces apoptosis and cell cycle arrest through activation of extracellular signal-regulated kinase and p38 mitogen-activated protein kinase pathways in human breast cancer cells. *The Journal of pharmacology and experimental therapeutics*, 313(1), 333-344.

Jhansi, D., & Kola, M. (2019). The antioxidant potential of Centella asiatica: A review. J. Med. Plants Stud, 7, 18-20.

Jo, D. H., Kim, J. H., Lee, T. G., & Kim, J. H. (2015). Size, surface charge, and shape determine therapeutic effects of nanoparticles on brain and retinal diseases. *Nanomedicine: Nanotechnology, Biology and Medicine*, 11(7), 1603-1611.

Kandasamy, A., Aruchamy, K., Rangasamy, P., Varadhaiyan, D., Gowri, C., Oh, T. H., Ramasundaram, S., & Athinarayanan, B. (2023). Phytochemical analysis and antioxidant activity of Centella asiatica extracts: an experimental and theoretical investigation of flavonoids. *Plants*, *12*(20), 3547.

Lian, G.-Y., Wang, Q.-M., Tang, P. M.-K., Zhou, S., Huang, X.-R., & Lan, H.-Y. (2018). Combination of asiatic acid and naringenin modulates NK cell anti-cancer immunity by rebalancing Smad3/Smad7 signaling. *Molecular Therapy*, 26(9), 2255-2266.

Macdonald, J. S. (1999). Toxicity of 5-fluorouracil. Oncology (Williston Park, NY), 13(7 Suppl 3), 33-34.

Manil, L., Mahieu, P., & Couvreur, P. (1995). Acute renal toxicity of doxorubicin (adriamycin)-loaded cyanoacrylate nanoparticles. *Pharmaceutical Research*, 12, 85-87.

Melekoğlu, A., Ekici, H., Esra, A., & Karahan, S. (2020). Evaluation of melamine and cyanuric acid cytotoxicity: an in vitro study on L929 fibroblasts and CHO cell line. *Ankara Üniversitesi Veteriner Fakültesi Dergisi*, 67(4), 399-406.

Moraru, C., Mincea, M., Menghiu, G., & Ostafe, V. (2020). Understanding the Factors Influencing Chitosan-Based Nanoparticles-Protein Corona Interaction and Drug Delivery Applications. *Molecules*, 25(20), 4758. <a href="https://www.mdpi.com/1420-3049/25/20/4758">https://www.mdpi.com/1420-3049/25/20/4758</a>

Németh, Z., Csóka, I., Semnani Jazani, R., Sipos, B., Haspel, H., Kozma, G., Kónya, Z., & Dobó, D. G. (2022). Quality by Design-Driven Zeta Potential Optimisation Study of Liposomes with Charge Imparting Membrane Additives. *Pharmaceutics*, 14(9). <a href="https://doi.org/10.3390/pharmaceutics14091798">https://doi.org/10.3390/pharmaceutics14091798</a>

Pang, H., Wu, H., Zhan, Z., Wu, T., Xiang, M., Wang, Z., Song, L., & Wei, B. (2024). Exploration of anti-osteosarcoma activity of asiatic acid based on network pharmacology and in vitro experiments. *Oncology Reports*, 51(2), 1-15.

Pantia, S., Kangsamaksin, T., Janvilisri, T., & Komyod, W. (2023). Asiatic acid inhibits nasopharyngeal carcinoma cell viability and migration via suppressing STAT3 and Claudin-1. *Pharmaceuticals*, 16(6), 902.

Pochapski, D. J., Carvalho dos Santos, C., Leite, G. W., Pulcinelli, S. H., & Santilli, C. V. (2021). Zeta Potential and Colloidal Stability Predictions for Inorganic Nanoparticle Dispersions: Effects of Experimental Conditions and Electrokinetic Models on the Interpretation of Results. *Langmuir*, 37(45), 13379-13389. <a href="https://doi.org/10.1021/acs.langmuir.1c02056">https://doi.org/10.1021/acs.langmuir.1c02056</a>

Qiu, Y., Liu, Y., Wang, L., Xu, L., Bai, R., Ji, Y., Wu, X., Zhao, Y., Li, Y., & Chen, C. (2010). Surface chemistry and aspect ratio mediated cellular uptake of Au nanorods. *Biomaterials*, 31(30), 7606-7619.

Rahman, M. M., Sayeed, M. S. B., Haque, M. A., Hassan, M. M., & Islam, S. (2012). Phytochemical screening, antioxidant, anti-Alzheimer and anti-diabetic activities of Centella asiatica. *J Nat Prod Plant Resour*, 2(4), 504-511.

Rai, N., Agrawal, R., & Khan, A. (2014). Centella asiatica extract exhibit anticancer activity against different types of tumours. *Int. J. Pure App. Biosci*, 2, 122-127.

Rauf, S., Hameed, H., Tariq, M., Afareen, A., Gulfaraz, S., AlKubaisi, N. A., & Elshikh, M. S. (2025). Phytochemical-Mediated Synthesis and Characterization of Silver Nanoparticles Using Mirabilis jalapa Leaf Extract and Their Antibacterial. *Microscopy Research and Technique*.

Razali, N. N. M., Ng, C. T., & Fong, L. Y. (2019). Cardiovascular protective effects of Centella asiatica and its triterpenes: a review. *Planta Medica*, 85(16), 1203-1215.

Rexroth, G., & Scotland, V. (1994). Cardiac toxicity of 5-fluorouracil. Medizinische Klinik (Munich, Germany: 1983), 89(12), 680-688

Rzayev, Z. M., Tűrk, M., & Söylemez, E. A. (2012). Bioengineering functional copolymers. XXI. Synthesis of a novel end carboxyltrithiocarbonate functionalized poly (maleic anhydride) and its interaction with cancer cells. *Bioorganic & Medicinal Chemistry*, 20(16), 5053-5061.

Sinmez, C. C., Tüfekçi, E., Demir, B. Ş., Eken, A., Guneş, V., Ekici, S., Bozkaya, E., & Aykun, A. İ. (2024). Investigation of immunomodulatory and cytotoxic effects of shed snake skin (Elaphe sauromates) extract. *Frontiers in Pharmacology*, 15, 1270970.

Soyingbe, O. S., Mongalo, N. I., & Makhafola, T. J. (2018). In vitro antibacterial and cytotoxic activity of leaf extracts of Centella asiatica (L.) Urb, Warburgia salutaris (Bertol. F.) Chiov and Curtisia dentata (Burm. F.) C.A.Sm - medicinal plants used in South Africa. *BMC Complementary and Alternative Medicine*, 18(1), 315. <a href="https://doi.org/10.1186/s12906-018-2378-3">https://doi.org/10.1186/s12906-018-2378-3</a>

Şahin, Y., Türk, M., Sevin, S., Peker, K., Bozkaya, E., Peker, S. A., & Çavdar, A. (2023). Cytotoxic and antiproliferative effects of hellebrin on breast and lung cancer cells. *Veteriner Hekimler Derneği Dergisi*, 94(2), 137-143.

Wiciński, M., Fajkiel-Madajczyk, A., Kurant, Z., Gajewska, S., Kurant, D., Kurant, M., & Sousak, M. (2024). Can Asiatic Acid from Centella asiatica Be a Potential Remedy in Cancer Therapy?—A Review. *Cancers*, 16(7), 1317.

Wu, T., Geng, J., Guo, W., Gao, J., & Zhu, X. (2017). Asiatic acid inhibits lung cancer cell growth in vitro and in vivo by destroying mitochondria. *Acta Pharm Sin B*, 7(1), 65-72. <a href="https://doi.org/10.1016/j.apsb.2016.04.003">https://doi.org/10.1016/j.apsb.2016.04.003</a>

Yırtıcı, Ü., Ergene, A., Adem, Ş., Atalar, M. N., Eyüpoğlu, V., Rawat, R., Arat, E., & Hamzaoğlu, E. (2024). Centaurea mersinensis phytochemical composition and multi-dimensional bioactivity properties supported by molecular modeling. *Journal of Biomolecular Structure and Dynamics*, 42(5), 2341-2357.

Zhang, T., Wang, L., Chen, Q., & Chen, C. (2014). Cytotoxic potential of silver nanoparticles. *Yonsei Med J*, 55(2), 283-291. https://doi.org/10.3349/ymj.2014.55.2.283

Zulkipli, N. N., Zakaria, R., Long, I., Abdullah, S. F., Muhammad, E. F., Wahab, H. A., & Sasongko, T. H. (2020). In silico analyses and cytotoxicity study of asiaticoside and asiatic acid from malaysian plant as potential mTOR inhibitors. *Molecules*, 25(17), 3991.